

ACCEPTED MANUSCRIPT • OPEN ACCESS

Declining Winter Heat Loss Threatens Continuing Ocean Convection at a Mediterranean Dense Water Formation Site

To cite this article before publication: Simon A. Josey *et al* 2022 *Environ. Res. Lett.* in press <https://doi.org/10.1088/1748-9326/aca9e4>

Manuscript version: Accepted Manuscript

Accepted Manuscript is “the version of the article accepted for publication including all changes made as a result of the peer review process, and which may also include the addition to the article by IOP Publishing of a header, an article ID, a cover sheet and/or an ‘Accepted Manuscript’ watermark, but excluding any other editing, typesetting or other changes made by IOP Publishing and/or its licensors”

This Accepted Manuscript is © 2022 The Author(s). Published by IOP Publishing Ltd.

As the Version of Record of this article is going to be / has been published on a gold open access basis under a CC BY 3.0 licence, this Accepted Manuscript is available for reuse under a CC BY 3.0 licence immediately.

Everyone is permitted to use all or part of the original content in this article, provided that they adhere to all the terms of the licence <https://creativecommons.org/licenses/by/3.0>

Although reasonable endeavours have been taken to obtain all necessary permissions from third parties to include their copyrighted content within this article, their full citation and copyright line may not be present in this Accepted Manuscript version. Before using any content from this article, please refer to the Version of Record on IOPscience once published for full citation and copyright details, as permissions may be required. All third party content is fully copyright protected and is not published on a gold open access basis under a CC BY licence, unless that is specifically stated in the figure caption in the Version of Record.

View the [article online](#) for updates and enhancements.

1
2
3 1
4
5 2 **Declining Winter Heat Loss Threatens Continuing Ocean Convection at a**
6
7 3 **Mediterranean Dense Water Formation Site**
8
9 4

10
11
12 5 Simon A. Josey¹ and Katrin Schroeder²
13
14 6
15 7
16 8
17 9
18 10
19 11
20 12

21 13 **Ocean-Atmosphere Interaction, Climate Change, Dense Water Formation**
22 14
23 15
24 16
25 17
26 18
27 19
28 20
29 21
30 22
31 23
32 24
33 25
34 26
35 27
36 28
37 29
38 30
39 31
40 32
41 33
42 34
43 35
44 36
45 37
46 38
47 39
48 40
49 41
50 42
51 43
52 44
53 45
54 46
55 47
56 48
57 49
58 50
59 51
60 52

20 **Affiliation:** 1) National Oceanography Centre, Southampton, UK. 2) Consiglio
21 Nazionale delle Ricerche, Istituto di Scienze Marine, Venice, Italy.

23 **Corresponding author:** Simon Josey (simon.josey@noc.ac.uk)
24

26 **Abstract**

27 A major change in winter sea surface heat loss between two key Mediterranean dense
28 water formation sites, the North-west Mediterranean (NWMed) and the Aegean Sea,
29 since 1950 is revealed using atmospheric reanalyses. The NWMed heat loss has
30 weakened considerably (from -154 Wm^{-2} in 1951-1985 to -137 Wm^{-2} in 1986-2020)
31 primarily because of reduced latent heat flux. This long-term weakening threatens
32 continued dense water formation, and we show by evaluation of historical observations
33 that winter-time ocean convection in the NWMed has declined by 40% from 1969 to
34 2018. Extension of the heat flux analysis reveals changes at other key dense water
35 formation sites that favour an eastward shift in the locus of Mediterranean convection
36 towards the Aegean Sea (where heat loss has remained unchanged at -172 Wm^{-2}). The
37 contrasting behaviour is due to differing time evolution of sea-air humidity and
38 temperature gradients. These gradients have weakened in the NWMed due to more
39 rapid warming of the air than the sea surface but remain near-constant in the Aegean.
40 The different time evolution reflects the combined effects of global heating and
41 atmospheric circulation changes which tend to offset heating in the Aegean but not the
42 NWMed. The shift in heat loss has potentially significant consequences for dense water
43 formation at these two sites and outflow to the Atlantic. Our observation of differential
44 changes in heat loss has implications for temporal variations in the balance of
45 convection elsewhere e.g., the Labrador-Irminger-Nordic Seas nexus of high latitude
46 Atlantic dense water formation sites.

47

48 **1. Introduction**

49 The Mediterranean Sea has experienced notable changes in many properties as a
50 result of the climate crisis (MedECC, 2020). These include warming and salinification

1
2
3 51 of intermediate (Schroeder et al., 2017; Margirier et al., 2020) and deep (Garcia-
4
5 52 Lafuente, 2021) water masses. Schroeder et al. (2017) found increasing temperature
6
7 53 and salinity of intermediate water crossing the Sicily Channel since the early 1990s
8
9 54 while Margirier et al. (2020) identified similar trends in the North-West Mediterranean
10
11 55 (NWMed hereafter) since 2007. Recently, Garcia-Lafuente et al. (2021) observed very
12
13 56 strong warming of deep Mediterranean outflow to the Atlantic since 2013.
14
15

16
17 57 Variations in the air-sea heat and freshwater fluxes that mediate these changes are
18
19 58 less well studied, particularly over multidecadal timescales. Here, we evaluate
20
21 59 Mediterranean winter heat loss variability since 1950 in regions of dense water
22
23 60 formation using the relatively high resolution ERA5 (0.25 x 0.25°, Hersbach et al.,
24
25 61 2020) reanalysis supplemented by the 20CRv3 reanalysis (0.7 x 0.7°, Slivinski et al.,
26
27 62 2019) which enables us to check for dataset consistency. We also assess the occurrence
28
29 63 of wintertime convection in the NWMed from 1969 to 2018 using historical
30
31 64 observations.
32
33

34
35 65 Severe winter heat loss leading to dense water formation has been observed at three
36
37 66 Mediterranean Sea sites: the NWMed, Northern Adriatic and Aegean Seas (e.g.
38
39 67 Schroeder et al., 2022). The NWMed was the first to be recognised in the Mediterranean
40
41 68 Ocean Convection (MEDOC) observing campaigns, undertaken from 1969-1972
42
43 69 (MEDOC Group, 1970) and has been the subject of many subsequent surveys. The
44
45 70 Eastern Mediterranean (EMed) has two deep water formation areas, the Adriatic Sea
46
47 71 (e.g. Malanotte-Rizzoli and Hecht, 1988) and the Aegean Sea which contributes less
48
49 72 regularly (Schroeder, 2019). The Adriatic is usually described as the main deep water
50
51 73 source for the EMed (Wüst, 1961; Schlitzer et al., 1991).
52
53

54
55 74 However, in the severe heat loss winters of 1991-1992 and 1992-1993 (Josey, 2003),
56
57 75 the Aegean took over and became the main EMed deep water formation site (Roether
58
59
60

1
2
3 76 et al., 1996). After 2002, the Adriatic gradually recovered as the main site (Ozer et al.,
4
5 77 2020; Manca et al., 2006; Rubino and Hainbucher, 2007; Bensi et al., 2013).
6
7 78 Knowledge of possible Aegean Sea dense water formation prior to the 1980s is severely
8
9 79 limited by lack of observations. Since 2000, more frequent observations are available
10
11 80 and new dense water production occurred in 2003, 2006-08, 2012, 2015 and 2017
12
13 81 (Androulidakis et al., 2012; Karageorgis et al., 2012; Velaoras et al., 2017, 2021;
14
15 82 Zervakis et al., 2019).

16
17
18
19 83 Our analysis will show both a multidecadal reduction of about 40% in the frequency
20
21 84 of NWMed convective winters and a major shift since 1950 in the balance of winter
22
23 85 surface heat loss between dense water formation sites in the western and eastern
24
25 86 Mediterranean. Specifically, NWMed heat loss weakens while Aegean heat loss
26
27 87 remains unchanged. In addition, we will show that the Adriatic Sea heat loss also
28
29 88 weakens but by a smaller amount than the NWMed; as the Adriatic change is smaller
30
31 89 we do not consider it in detail. The reasons for the strong contrast between the NWMed
32
33 90 and Aegean will be determined by analysing the heat flux components and atmospheric
34
35 91 variables driving the heat loss. Since the NWMed is the region experiencing the strong
36
37 92 winter heat loss change, it is the primary focus of our study and we contrast it with the
38
39 93 Aegean but do not consider the latter region in such detail as it has not undergone a
40
41 94 major change. Finally, we discuss the implications of our results and place them in the
42
43 95 context of recent research which suggests that NWMed dense water formation may
44
45 96 cease in the next 20-30 years (Parras-Berrocal et al, 2022).

46
47
48
49
50
51 97

52 53 98 **2. Methods**

54
55 99 We employ monthly mean surface heat exchange, near surface meteorology and sea
56
57 100 surface temperature fields from ERA5 and 20CRv3. Near surface variables are
58
59
60

101 specified at 2 m for temperature and humidity and 10 m for wind speed. The net heat
 102 flux (Q_n) is the sum of latent (Q_e), sensible (Q_h), shortwave (Q_{sw}) and longwave (Q_{lw})
 103 components:

$$104 \quad Q_n = Q_e + Q_h + Q_{lw} + Q_{sw} \quad (1)$$

105 The sign convention is for ocean heat gain/loss to be positive/negative. Winter is
 106 defined to be December-February when latent and sensible heat fluxes dominate net
 107 heat flux variability.

108 These fluxes are dependent on near surface gradients of humidity (for latent) and
 109 temperature (for sensible) together with the wind speed through the following formulae:

$$110 \quad Q_e = \rho L C_e u (q_s - q_a) \quad (2)$$

$$112 \quad Q_h = \rho c_p C_h u (T_s - T_a) \quad (3)$$

113 Here, ρ is air density; L , latent heat of vaporisation; C_e and C_h , latent and sensible heat
 114 transfer coefficients; u , wind speed; q_s , 98% of saturation specific humidity at sea
 115 surface temperature; q_a , near surface atmospheric specific humidity; c_p , specific heat
 116 capacity of air at constant pressure; T_s , sea surface temperature (SST); T_a , near surface
 117 air temperature. Units employed for the variables discussed in this manuscript are heat
 118 flux (Wm^{-2}), wind speed (ms^{-1}), humidity ($g\ kg^{-1}$), temperature ($^{\circ}C$).

119

120 **3. Results**

121 3.1 Spatial Structure of Winter Heat Loss

122 We begin by exploring the structure of the mean winter heat loss and its interannual
 123 variability within the high resolution ERA5 dataset. The Mediterranean experiences

1
2
3 124 ocean heat loss in winter (Fig.1a), with relatively weak loss (-50 Wm^{-2}) in the Alboran
4
5 125 Sea, intermediate values (-100 Wm^{-2}) over most of the basin (e.g., the Ionian and
6
7 126 Levantine Seas) and strong loss (reaching -200 Wm^{-2}) in the NWMed, Adriatic and
8
9 127 Aegean Seas. ERA5 reveals finer scale spatial structure than was evident using earlier
10
11 128 coarser resolution datasets (e.g., Josey, 2003). In particular, an east-west gradient of
12
13 129 strengthening heat loss is evident in the Aegean Sea with highest values in the eastern
14
15 130 Aegean.

16
17
18
19 131 Climatological winter mean values for the net heat flux and its components in the
20
21 132 NWMed and Aegean are provided in Table 1. For each region, the largest term is the
22
23 133 latent flux (-115 Wm^{-2} of -146 Wm^{-2} net heat loss in the NWMed and -135 Wm^{-2} of -
24
25 134 172 Wm^{-2} in the Aegean) reinforced by the sensible flux (-30 Wm^{-2} in the NWMed, -
26
27 135 46 Wm^{-2} in the Aegean). In the NWMed, the longwave loss is about equal and opposite
28
29 136 in sign to the shortwave gain so these terms cancel. In the Aegean, shortwave gain
30
31 137 exceeds longwave loss by about 10 Wm^{-2} resulting in a small net gain which reduces
32
33 138 slightly the strong losses from Q_e and Q_h .

34
35
36
37 139 To provide context for the multidecadal variability which is the focus of our study,
38
39 140 we first briefly consider the spatial structure of interannual variability of winter Q_n
40
41 141 (Fig.1b). The variability is strongest, approaching 50 Wm^{-2} , in the NWMed and Aegean
42
43 142 Seas. In contrast, Adriatic Sea variations are noticeably weaker, typically $30\text{-}35 \text{ Wm}^{-2}$,
44
45 143 indicating it experiences steady winter heat loss. The vectors show stronger wind
46
47 144 forcing of the Aegean and NWMed than the Adriatic. Fluctuations in these winds and
48
49 145 the associated air mass temperature and humidity are the source of the strong
50
51 146 interannual variability via Q_e and Q_h .

52
53
54
55
56 147

57
58 148 3.2 Multidecadal Variability of Heat Loss and Winter Convection
59
60

1
2
3 149 Turning to multidecadal variability, we find that winter heat loss in the NWMed
4
5 150 exhibits a striking long-term weakening from -154 ± 6 Wm^{-2} in 1951-1985 to -137 ± 6
6
7 151 Wm^{-2} in 1986-2020 (Fig.2a). There is still notable interannual to decadal variability
8
9 152 within this period so this weakening should not necessarily be regarded as a smooth
10
11 153 linear change (see Supp Fig.1 and discussion). The long-term reduction in winter heat
12
13 154 loss will in turn weaken the surface buoyancy loss and thereby threaten convection in
14
15 155 the NWMed. With this in mind, we have assessed hydrographic survey observations
16
17 156 from 1969 to 2018 and identified the number of convective winters in each decade in
18
19 157 this period (Table 2). The first two decades (1969-1988) have 14 convective winters
20
21 158 compared with 13 in the subsequent three decades (1989-2018). Thus, there has been a
22
23 159 multidecadal reduction of about 40% in the frequency of NWMed convective winters
24
25 160 from 7 per decade to just over 4 per decade. This is consistent with a scenario in which
26
27 161 reduced winter heat loss has inhibited convection in recent decades (assessment of
28
29 162 convection in the early reanalysis record from 1950-68 is not possible due to lack of
30
31 163 observations). We have also carried out an assessment, based on available literature to
32
33 164 date, of the four additional winters 2019 through to 2022 and find no evidence for deep
34
35 165 convection in these winters. Thus, there are no reports of deep convection in the
36
37 166 NWMed for the last 9 winters (2014-2022 inclusive) which suggests that cessation of
38
39 167 deep convection in the NW Mediterranean may have already begun. The previous
40
41 168 biggest gaps in the record going back to 1969 were 4 winters (1995-1998 and 2001-
42
43 169 2004).

44
45 170 In contrast to the NWMed, the Aegean Sea net heat flux (Fig.2b) has remained
46
47 171 unchanged over the past 70 years with winter mean values of -171 ± 6 Wm^{-2} in 1951-
48
49 172 1985 and -172 ± 6 Wm^{-2} in 1986-2020. As noted in the Introduction, the number of
50
51 173 available historical hydrographic surveys in the Aegean region is much lower than for
52
53
54
55
56
57
58
59
60

1
2
3 174 the NWMed and this prevents us from undertaking a similar evaluation for the Aegean
4
5 175 to that reported in Table 2. However, given the unchanged Aegean Sea mean winter
6
7 176 heat loss values between the two periods reported above, we expect the potential for
8
9 177 convection in the Aegean Sea to be unaffected by the winter heat loss regime unlike the
10
11 178 NWMed. Note, we also examined Q_n variability in the Adriatic (using region 41-43 °N,
12
13 179 14-20 °E) and find weakening from $-147 \pm 5 \text{ Wm}^{-2}$ in 1951-1985 to $-133 \pm 5 \text{ Wm}^{-2}$ in
14
15 180 1986-2020. Thus, the Adriatic also experiences, at a slightly lower level, the reduction
16
17 181 in heat loss found in the NWMed.
18
19
20

21
22 182 We have tested whether the reported multidecadal variability is sensitive to the
23
24 183 choice of dataset by repeating the analysis with 20CRv3. The corresponding 20CRv3
25
26 184 time series are in close agreement with ERA5 ($r^2=0.95/0.93$ and rms difference= $8.8/8.7$
27
28 185 Wm^{-2} for NWMed/Aegean) so the observed variability is robust to the choice of
29
30 186 reanalysis employed (Fig. 2a-b). Temporal inhomogeneity arising from assimilation of
31
32 187 multiple data types is a potentially significant problem for reanalyses. As 20CRv3 only
33
34 188 assimilates sea level pressure, these results indicate that inhomogeneity issues do not
35
36 189 seriously impact the representation of variability by ERA5. We also note that we have
37
38 190 employed a preliminary version of the ERA5 back extension for the period 1950-1978
39
40 191 ([https://confluence.ecmwf.int/display/CKB/ERA5%3A+data+documentation#ERA5:
41
42 192 datadocumentation-Dataupdatefrequency](https://confluence.ecmwf.int/display/CKB/ERA5%3A+data+documentation#ERA5:datadocumentation-Dataupdatefrequency)). The close agreement with 20CRv3 is
43
44 193 indicative that the ERA5 back extension is not strongly affected by unrealistic
45
46 194 variability but a further check using the final ERA5 back extension would be
47
48 195 worthwhile when it becomes available. Finally, to examine whether the form of the heat
49
50 196 loss distribution has changed, we consider distributions of NWMed and Aegean
51
52 197 individual winter month Q_n at grid cell level which have been generated using all ERA5
53
54 198 grid cells within each region (Fig.2c-d). The NWMed distribution clearly shows the
55
56
57
58
59
60

199 shift towards weaker heat loss with a reduction/increase in the number of grid cells
200 experiencing Q_n stronger/weaker than about -130 Wm^{-2} . The corresponding Aegean
201 distribution has remained largely unaltered with some indication of a slight narrowing.

202 Our focus is multidecadal variability but considering interannual variability briefly,
203 we remark that the severe 1991-1992 and 1992-1993 Aegean heat loss winters are
204 clearly evident in Fig.2b in both ERA5 and 20CRv3. In this context, we note that a pair
205 of successive extreme heat loss winters was also observed in the subpolar North
206 Atlantic in 2013-14 and 2014-15 (Josey et al., 2018, 2022). It is possible that such
207 paired severe winters are becoming more frequent and in subsequent work it would be
208 interesting to explore whether they have common causal processes (e.g., second severe
209 winter triggered by ocean feedback to the atmosphere via re-emergence of first winter
210 temperature anomalies sequestered below the mixed layer in the intervening summer).

211 212 3.3 Drivers of Multidecadal Change

213 Decomposition into component terms reveals that the NWMed Q_n weakening is
214 due primarily to weaker Q_e and Q_h with an additional small contribution from stronger
215 Q_{sw} (Fig.3). Specifically, Q_e is $8\pm 3 \text{ Wm}^{-2}$ weaker in 1986-2020 compared to 1951-1985,
216 with Q_h weakening by $6\pm 2 \text{ Wm}^{-2}$ and Q_{sw} increasing by $4\pm 1 \text{ Wm}^{-2}$. In contrast, the
217 Aegean Sea Q_e and Q_h values are the same to within 2 Wm^{-2} in both periods and there
218 are small compensating changes in the radiative (Q_{sw} , Q_{lw}) terms which leave Q_n
219 essentially unchanged through the past 70 years.

220 Q_e (Q_h) is strongly influenced by the humidity (temperature) gradient between the
221 sea surface and near surface atmosphere (Equations 2-3) and the wind speed. Winter
222 mean temperature, humidity and wind speed for 1950-2020 are listed in Table 1. In
223 each region, the sea surface is warmer than the near surface atmosphere in winter, with

1
2
3 224 $\Delta T = 2.1$ (3.0) °C, in the NWMed (Aegean). Likewise, the gradient in humidity is
4
5 225 positive with $\Delta q = 3.5$ (4.1 g kg⁻¹). Wind speed values are similar between the two
6
7 226 regions, $u=7.5$ (7.1) m s⁻¹, in the NWMed (Aegean).
8
9

10 227 Changes in the values of these terms in 1986-2020 relative to 1951-1985 are shown
11
12 228 in Fig.3a-b (wind speed) and Fig. 3c-d (temperature and humidity terms). The NWMed
13
14 229 weakening of Q_e (Q_h) is seen to correspond to a reduction in the driving Δq (ΔT)
15
16 230 gradients due to $q_a(T_a)$ increasing more than $q_s(T_s)$ (Fig.3c). Specifically, T_a increases
17
18 231 by 0.50 °C from 11.12 °C (1951-1985) to 11.62 °C (1986-2020) while T_s only increases
19
20 232 by 0.15 °C from 13.41 °C to 13.56 °C and so ΔT falls by 0.35 °C i.e. the sea-air
21
22 233 temperature difference weakens. Similar behaviour is observed for humidity with Δq
23
24 234 weakening by 0.12 g kg⁻¹. In contrast, the ΔT and Δq changes in the Aegean are small
25
26 235 (Fig.3d). Here, T_a and T_s increase by 0.16 °C and 0.09 °C respectively so the reduction
27
28 236 in ΔT is only 0.07 °C i.e. the Aegean sea-air temperature difference is essentially
29
30 237 unchanged in contrast to the 0.35 °C reduction in the NWMed. Likewise, Δq is virtually
31
32 238 unchanged in the Aegean.
33
34
35
36

37 239 There is also the potential for wind speed (u) changes to influence Q_e and Q_h .
38
39 240 However, changes in u are similar between the NWMed and Aegean so they are not
40
41 241 responsible for the different Q_n changes over the past 70 years. In the NWMed, u falls
42
43 242 slightly from 7.6 ± 0.1 m s⁻¹ in 1951-85 to 7.3 ± 0.1 m s⁻¹ in 1986-2020 while in the
44
45 243 Aegean the corresponding change is also a slight reduction from 7.1 ± 0.1 to 6.9 ± 0.1 m
46
47 244 s⁻¹.
48
49

50
51 245 We now investigate why the near surface air temperature and humidity have
52
53 246 increased more rapidly in the NWMed than the Aegean. One possibility is that global
54
55 247 heating is being modulated by regional changes in atmospheric circulation such that the
56
57 248 heating is offset in the Aegean or amplified in the NW Med. The change between 1951-
58
59
60

1
2
3 249 1985 and 1986-2020 of ERA5 winter mean T_a and u are shown in Fig.4a. A broad
4
5 250 pattern of warming is evident with increases over the sea typically 0.2-0.5 °C and larger
6
7 251 values over land (0.5-1.0 °C). The T_a increase in the NWMed is greater than in the
8
9 252 Aegean, consistent with our results noted above (note the near surface humidity shows
10
11 253 a similar contrast between these two regions, Fig. SF2). The wind field reveals a
12
13 254 strengthened northerly airflow over the Aegean while the NWMed experiences just a
14
15 255 small, localised change. This difference may partly explain the East-West gradient in
16
17 256 the strength of the warming. Specifically, the global heating signal in the Aegean may
18
19 257 be partially offset by the increased northerly airflow which is cooler because of the
20
21 258 climatological north-south gradient in air temperature. We propose that this
22
23 259 combination of pervasive global heating and regional cooling due to atmospheric
24
25 260 circulation changes has the potential to lead to the observed differential changes in the
26
27 261 strength of winter heat loss (and thus potential for dense water formation) in the
28
29 262 NWMed and Aegean.
30
31
32
33
34
35
36
37
38
39

264 **4. Discussion and Conclusions**

40 265 The Mediterranean Sea is one of the few regions of the global ocean that provides
41
42 266 the opportunity to investigate winter surface heat loss in regions of dense water
43
44 267 formation. Previous research has considered extreme winter heat loss (e.g. Josey, 2003;
45
46 268 Schroeder et al., 2010; Velaoros et al., 2017) and recent trends which now register the
47
48 269 impacts of the climate crisis (Garcia-Lafuente, 2021). Our focus is multidecadal
49
50 270 variability in the NWMed and Aegean. We find a major change in winter heat loss. In
51
52 271 the NWMed, heat loss has weakened by 17 Wm^{-2} (from -154 Wm^{-2} in 1951-1985 to -
53
54 272 137 Wm^{-2} in 1986-2020) primarily because of latent and sensible heat reductions. A
55
56 273 similar but slightly smaller reduction of 14 Wm^{-2} is found in the Adriatic. In contrast,
57
58
59
60

1
2
3 274 the Aegean heat loss has remained unchanged. The different NWMed and Aegean
4
5 275 variability is mainly due to changes in the sea-air humidity and temperature gradients.
6
7 276 These gradients have weakened since 1950 in the NWMed due to more rapid warming
8
9 277 of the near surface atmosphere than the sea surface. The corresponding gradients in the
10
11 278 Aegean have remained near constant. This difference may reflect regional circulation
12
13 279 cooling of Aegean air temperature that potentially offsets pervasive background global
14
15 280 heating. Further research with Mediterranean climate models is needed to test this
16
17 281 suggestion.
18
19
20

21 282 The strong reduction in NWMed heat loss will impact the buoyancy flux and thus
22
23 283 threaten continued winter convection in this region. We have tested whether this is
24
25 284 evident in the hydrographic record and find that number of convective winters has fallen
26
27 285 from 18 in the first half (1969-1995) of the period since reliable hydrographic
28
29 286 observations began to 9 in the second half (1996-2022). So, we suggest that the
30
31 287 multidecadal decline in severity of NWMed winter heat loss is linked to a
32
33 288 corresponding decline in convection and thus new dense water formation. We also find
34
35 289 that there are no reports of deep convection in the NWMed for the last nine winters
36
37 290 (2014-2022 inclusive) which suggests that cessation of deep convection in the NW
38
39 291 Mediterranean may have already begun. We note that previous studies have produced
40
41 292 mixed results for changes to the Mediterranean heat flux, with no consistent evidence
42
43 293 for significant trends (Dubois et al., 2012; Nabat et al., 2014; Sevault et al., 2014;
44
45 294 Somot et al., 2018) apart from Mariotti (2010). These studies have employed models
46
47 295 as well as observation-based datasets and typically considered shorter periods than the
48
49 296 one we have considered with a tendency to focus on basin scale budgets rather than
50
51 297 regional variations. Of particular interest is the study of Somot et al. (2018) which does
52
53 298 have a regional focus and explores in detail the processes controlling interannual
54
55
56
57
58
59
60

1
2
3 299 variability of deep water formation in the NW Med. They find no trend in either the net
4
5 300 heat flux or the number of convective winters but this may reflect the shorter period
6
7 301 used for their analysis (1980-2013).
8
9

10 302 A schematic summary of our findings is shown in Fig. 4b. In the NWMed, T_a has
11
12 303 increased by substantially more than T_s , leading to a reduction in sea-air temperature
13
14 304 difference; similarly for the humidity variables (not shown). In turn, the reduction in
15
16 305 ΔT and Δq weakens NWMed heat loss as these gradients are drivers of Q_e and Q_h .
17
18 306 Consequently, we expect a multidecadal reduction in NWMed convection as observed.
19
20 307 In contrast, the Aegean T_a increase is only slightly larger than T_s , so the sea-air
21
22 308 temperature difference and winter heat loss in this region are largely unchanged. The
23
24 309 regional change in atmospheric circulation which we suggest may have brought colder
25
26 310 air from the north to the Aegean, partially offsetting the pervasive global heating
27
28 311 increase is also shown in Fig.4b. The background sea level pressure change field in the
29
30 312 figure shows that the NWMed has experienced a multidecadal increase in pressure
31
32 313 while the Aegean is positioned such that the pressure change favours an enhanced
33
34 314 northerly flow in winter. Additional research is required to establish the consequences
35
36 315 for Mediterranean Sea dense water formation and circulation. Such changes have the
37
38 316 potential to impact the properties of the water outflowing to the Atlantic through the
39
40 317 Strait of Gibraltar which is difficult to represent in climate models (Behr et al., 2022).
41
42 318 The potential for differential changes in heat loss, driven by a combination of global
43
44 319 warming and regional atmospheric circulation anomalies, also has implications for
45
46 320 temporal variations in the balance of convection elsewhere. In particular, the Labrador-
47
48 321 Irminger-Nordic Seas nexus of high latitude Atlantic dense water formation sites is
49
50 322 known to be sensitive to changes in the regional atmospheric circulation (e.g., Josey et
51
52
53
54
55
56
57
58
59
60

1
2
3 323 al., 2019; Kenigson and Timmermans, 2021) and the combination of such changes with
4
5 324 the background effects of global heating merits investigation.
6
7

8 325 Our results are relevant to studies of future changes in Mediterranean Sea dense
9
10 326 water formation (Somot et al., 2006; Adloff et al., 2015; Soto-Navarro et al., 2020;
11
12 327 Amitai et al., 2021; Parras-Berrocal et al., 2022). Parras-Berrocal et al. (2022) recently
13
14 328 found using a high-resolution regional climate model that dense water formation in the
15
16 329 NWMed collapses by 2040-2050 primarily due to stronger vertical stratification. We
17
18 330 have found from a multidecadal observation-based analysis that weakening NWMed
19
20 331 heat loss is likely to have already played a role in limiting dense water formation. It is
21
22 332 worth stressing that the relative roles of these two processes (weakening heat loss,
23
24 333 stronger stratification) and the potential for possible mutual dependence have not yet
25
26 334 been explored. Indeed, determining their relative contributions to declining NWMed
27
28 335 dense water formation is likely to form a major challenge for the community in the
29
30 336 years ahead. Further work is needed to integrate the post-1950 weakening identified
31
32 337 here, with studies of post-2000 changes (Garcia-Lafuente et al., 2021) and projections
33
34 338 over the 21st century (e.g. Parras-Berrocal et al., 2022). The reduction in heat loss that
35
36 339 we have identified threatens ongoing convection in the NWMed and is a potential
37
38 340 contributory factor to the collapse of dense water formation in this region projected to
39
40 341 occur in the decades ahead.
41
42
43
44
45
46
47
48

49 343 **Acknowledgements**

50
51 344 SJ would like to acknowledge funding from the UK Natural Environment Research
52
53 345 Council.
54
55
56
57
58
59
60

1
2
3 348 **Data Availability Statement**
4

5 349 The data that support the findings of this study are openly available. See the
6
7 following sites for details:
8
9

10 351 ERA5 reanalysis - [https://cds.climate.copernicus.eu/cdsapp#!/dataset/reanalysis-
12 era5-single-levels-monthly-means?tab=overview](https://cds.climate.copernicus.eu/cdsapp#!/dataset/reanalysis-
11 era5-single-levels-monthly-means?tab=overview)
13

14 353 20CRv3 reanalysis - https://psl.noaa.gov/data/gridded/data.20thC_ReanV3.html.
15
16
17
18
19
20
21
22
23
24
25
26
27
28
29
30
31
32
33
34
35
36
37
38
39
40
41
42
43
44
45
46
47
48
49
50
51
52
53
54
55
56
57
58
59
60

355 **References**

- 356 Adloff, F., Somot, S., Sevault, F., Jordà, G., Aznar, R., & Déqué, M. (2015).
357 Mediterranean Sea response to climate change in an ensemble of twenty first century
358 scenarios. *Clim. Dyn.* **45**, 2775–2802, <https://doi.org/10.1007/s00382-015-2507-3>.
- 359 Amitai, Y., Ashkenazy, Y., & Gildor, H. (2021). The effect of the source of deep water
360 in the Eastern Mediterranean on Western Mediterranean intermediate and deep water.
361 *Frontiers in Marine Science*, 7, 615975. <https://doi.org/10.3389/fmars.2020.615975>.
- 362 Androulidakis, Y.S., Kourafalou, V. H., Krestenitis, Y. N. & V. Zervakis (2012).
363 Variability of deep water mass characteristics in the North Aegean Sea: the role of
364 lateral inputs and atmospheric conditions. *Deep Sea Res Part I Oceanogr Res Papers*
365 *67:55–72*. <https://doi.org/10.1016/j.dsr.2012.05.004>.
- 366 Behr, L., Luther, N., Josey, S. A., Luterbacher, J., Wagner, S. & Xoplaki, E. (2022).
367 On the representation of Mediterranean Overflow Waters in Global Climate Models, *J.*
368 *Phys. Oceanogr.*, doi: 10.1175/JPO-D-21-0082.1.
- 369 Bensi, M., Cardin, V., Rubino, A., Notarstefano, G. & Poulain, P. M., (2013). Effects
370 of winter convection on the deep layer of the Southern Adriatic Sea in 2012, *J. Geophys.*
371 *Res. Oceans*, 118, 6064–6075, doi:10.1002/2013JC009432.
- 372 Dubois C., Somot S., Calmanti S., Carillo A., Déqué M., et al. (2012) Future projections
373 of the surface heat and water budgets of the Mediterranean sea in an ensemble of
374 coupled atmosphere-ocean regional climate models, *Clim. Dyn.* 39 (7-8):1859-1884.
375 DOI 10.1007/s00382-011-1261-4.
- 376 García-Lafuente, J., Sammartino, S., Huertas, I. E, Flecha, S., Sánchez-Leal, R. F.,
377 Naranjo, C., et al., (2021). Hotter and Weaker Mediterranean Outflow as a Response to
378 Basin-Wide Alterations. *Front. Mar. Sci.* 8:613444. doi: 10.3389/fmars.2021.613444.

- 1
2
3 379 Gascard, J.-C. (1973). Vertical motions in a region of deep water formation. *Deep Sea*
4
5 380 *Research and Oceanographic Abstracts*, 20(11), 1011–1027.
6
7
8 381 Hersbach, H., Bell, B., Berrisford, P., Hirahara, S., Horányi, A., Muñoz-Sabater, J., et
9
10 382 al., (2020). The ERA5 Global Reanalysis. *Q. J. Roy. Met. Soc.* **146**, 1999.
11
12 383 Josey, S. A., (2003). Changes in the Heat and Freshwater Forcing of the Eastern
13
14 384 Mediterranean and their Influence on Deep Water Formation, *Journal of Geophysical*
15
16 385 *Research*, **108**(C7), 3237, doi:10.1029/2003JC001778.
17
18
19 386 Josey, S. A., Hirschi, J. J.-M., Sinha, B., Duchez, A., Grist, J. P. & Marsh, R. (2018).
20
21 387 The Recent Atlantic Cold Anomaly: Causes, Consequences and Related Phenomena,
22
23 388 *Annual Reviews of Marine Science*, doi.org/10.1146/annurev-marine-121916-063102.
24
25
26 389 Josey, S. A., M. F. de Jong, M. Oltmanns, G. K. Moore and R. A. Weller (2019).
27
28 390 Extreme Variability in Irminger Sea Winter Heat Loss Revealed by Ocean
29
30 391 Observatories Initiative Mooring and the ERA5 Reanalysis, *Geophys. Res. Lett.*,
31
32 392 <https://doi.org/10.1029/2018GL080956>.
33
34
35 393 Josey, S. A. & Sinha, B. (2022). Sub-Polar Atlantic Ocean Mixed Layer Heat Content
36
37 394 Variability is Increasingly Driven by an Active Ocean, *Nature Communications Earth*
38
39 395 *and Environment*, 10.1038/s43247-022-00433-6.
40
41
42 396 Karageorgis, A. P., Georgopoulos, D., Kanellopoulos, T. D., Mikkelsen, O. A., Pagou,
43
44 397 K., H. Kontoyiannis, et al. (2012). Spatial and seasonal variability of particulate matter
45
46 398 optical and size properties in the eastern Mediterranean Sea. *J Mar Syst* 105–108:123–
47
48 399 134. <https://doi.org/10.1016/j.jmarsys.2012.07.003>.
49
50
51 400 Kenigson, J. S. & Timmermans, M.-L. (2021). Nordic Seas Hydrography in the Context
52
53 401 of Arctic and North Atlantic Ocean Dynamics. *J. Phys. Oceanogr.*, 10.1175/JPO-D-20-
54
55 402 0071.1.

- 1
2
3 403 Malanotte-Rizzoli, P. & Hecht, A. (1988). Large-scale properties of the eastern
4
5 404 Mediterranean - A review. *Oceanologica Acta*, 11(4), 323-335.
6
7
8 405 Manca, B. B., Ibello, V., Pacciaroni, M., Scarazzato, P., & Giorgetti, A. (2006).
9
10 406 Ventilation of deep waters in the Adriatic and Ionian Seas following changes in
11
12 407 thermohaline circulation of the Eastern Mediterranean. *Climate Research*, 31, 239.
13
14 408 Margirier, F., Testor, P., Heslop, E., Mallil, K., Bosse, A., Houpert, L., et al. (2020).
15
16 409 Abrupt warming and salinification of intermediate waters interplays with decline of
17
18 410 deep convection in the Northwestern Mediterranean Sea. *Scientific Reports*, 10, 20923.
19
20 411 <https://doi.org/10.1038/s41598-020-77859-5>.
21
22
23 412 Mariotti, A. (2010). Recent changes in the Mediterranean water cycle: a pathway
24
25 413 toward long-term regional hydroclimatic change?. *Journal of Climate*, 23(6), 1513-
26
27 414 1525. MedECC (2020). *Climate and Environmental Change in the Mediterranean Basin*
28
29 415 – Current Situation and Risks for the Future. First Mediterranean Assessment Report
30
31 416 [Cramer, W., Guiot, J., Marini, K. (eds.)] Union for the Mediterranean, Plan Bleu,
32
33 417 UNEP/MAP, Marseille, France, 632pp. DOI: 10.5281/zenodo.4768833.
34
35 418 MEDOC Group (1970). Observation of Formation of Deep Water in the Mediterranean
36
37 419 Sea, 1969. *Nature* **227**, 1037–1040 (1970). <https://doi.org/10.1038/2271037a0>.
38
39 420 Mertens, C. & Schott, F., (1998). Interannual variability of deep-water formation in the
40
41 421 northwestern Mediterranean. *Journal of Physical Oceanography* 28, 1410–1424.
42
43 422 <https://doi.org/10.1175/1520-0485>.
44
45 423 Nabat P., Somot S., Mallet M., Sanchez-Lorenzo A. and Wild M. (2014) Contribution
46
47 424 of anthropogenic sulfate aerosols to the changing Euro-Mediterranean climate since
48
49 425 1980. *Geophys. Res. Lett.*, 41(15), 5605–5611, doi:10.1002/2014GL060798.
50
51 426 Ozer, T., Gertman, I., Gildor, H., Goldman, R. & Herut, B. (2020). Evidence for recent
52
53 427 thermohaline variability and processes in the deep water of the Southeastern Levantine
54
55
56
57
58
59
60

- 1
2
3 428 Basin, Mediterranean Sea. *Deep-Sea Research Part II*, 171, 104651.
4
5 429 <https://doi.org/10.1016/j.dsr2.2019.104651>.
6
7
8 430 Parras-Berrocal, I. M., Vázquez, R., Cabos, W., Sein, D. V., Ivarez, O., Bruno, M., &
9
10 431 Izquierdo, A. (2022). Surface and intermediate water changes triggering the future
11
12 432 collapse of deep water formation in the North Western Mediterranean. *Geophysical*
13
14 433 *Research Letters*, 49, e2021GL095404. <https://doi.org/10.1029/2021GL095404>.
15
16
17 434 Pinardi, N., Zavatarelli, M., Adani, M., Coppini, G., Fratianni, C., Oddo, P., et al.,
18
19 435 (2015). Mediterranean Sea large-scale low-frequency ocean variability and water mass
20
21 436 formation rates from 1987 to 2007: A retrospective analysis. *Progress in Oceanography*
22
23 437 132, 318–332, <https://doi.org/10.1016/j.pocean.2013.11.003>.
24
25
26 438 Rhein, M., (1995). Deep water formation in the western Mediterranean. *Journal of*
27
28 439 *Geophysical Research* 100, 6943–6959, <https://doi.org/10.1029/94JC03198>.
29
30
31 440 Roether, W., Manca, B. B, Klein, B., Bregant, D., Georgopoulos, D., Beitzel, V., et al.,
32
33 441 (1996). Recent changes in eastern Mediterranean deep waters. *Science*, 271:333–335.
34
35 442 Rubino, A. & D. Hainbucher (2007). A large abrupt change in the abyssal water masses
36
37 443 of the eastern Mediterranean, *Geophys. Res. Lett.*, 34, L23607,
38
39 444 [doi:10.1029/2007GL031737](https://doi.org/10.1029/2007GL031737).
40
41
42 445 Schlitzer, R., Roether, W., Oster, H., Junghans, H.-G., Hausmann, M., Johannsen, H.,
43
44 446 & Michelato, A. (1991). Chlorofluoromethane and oxygen in the Eastern
45
46 447 Mediterranean. *Deep-Sea Research*, 38, 12, 1531-1551.
47
48
49 448 Schott, F., Leaman, K. D. & Zika, R. G., (1988). Deep mixing in the Gulf of Lions,
50
51 449 Revisited. *Geophysical Research Letters* 15, 800–803,
52
53 450 <https://doi.org/10.1029/GL015i008p00800>
54
55
56
57
58
59
60

- 1
2
3 451 Schroeder, K. (2019). Current Systems in the Mediterranean Sea. In Cochran, J. Kirk;
4
5 452 Bokuniewicz, J. Henry; Yager, L. Patricia (Eds.) Encyclopedia of Ocean Sciences, 3rd
6
7 453 Edition. vol. 3, pp. 219-227, Elsevier. ISBN: 978-0-12-813081-0.
8
9
10 454 Schroeder, K., Chiggiato, J., Josey, S. A., Borghini, M., Aracri, S. & Sparnocchia, S.,
11
12 455 (2017). Rapid response to climate change in a marginal sea, Nature Scientific Reports,
13
14 456 7: 4065, DOI:10.1038/s41598-017-04455-5.
15
16
17 457 Schroeder, K., Josey, S. A., Herrmann, M., Grignon, L., Gasparini, G. P. & Bryden, H.
18
19 458 L. (2010). Abrupt warming and salting of the Western Mediterranean Deep Water:
20
21 459 atmospheric forcings and lateral advection, Journal of Geophysical Research, 115,
22
23 460 C08029, doi:10.1029/2009JC005749.
24
25
26 461 Schroeder, K., T. Tanhua, J. Chiggiato, D. Velaoras, S. A. Josey, J. G. Lafuente and M.
27
28 462 Vargas-Yanez, 2022: The forcings of the Mediterranean Sea and the physical properties
29
30 463 of its water masses, in 'Oceanography of the Mediterranean Sea', Elsevier, eds. K.
31
32 464 Schroeder and J. Chiggiato, p.93-123. Sevault F., Somot S., Alias A., Dubois C.,
33
34 465 Lebeaupin-Brossier C., et al. (2014) A fully coupled Mediterranean regional climate
35
36 466 system model: design and evaluation of the ocean component for the 1980-2012 period.
37
38 467 Tellus A, 66, 23967, <http://dx.doi.org/10.3402/tellusa.v66.23967>
39
40
41 468 Slivinski, L. C., Compo, G. P., Whitaker, J. S., Sardeshmukh, P. D., Giese, B. S.,
42
43 469 McColl, C. et al., (2019). Towards a more reliable historical reanalysis: Improvements
44
45 470 for version 3 of the Twentieth Century Reanalysis system. Quart. J. Roy. Meteor. Soc.,
46
47 471 145, 2876–2908, <https://doi.org/10.1002/qj.3598>.
48
49
50 472 Somot, S., Sevault, F., & Déqué, M., (2006). Transient climate change scenario
51
52 473 simulation of the Mediterranean Sea for the 21st century using a high-resolution ocean
53
54 474 circulation model. Climate Dynamics, 27, 851–879.
55
56
57
58
59
60

- 1
2
3 475 Somot, S., Houpert, L., Sevault, F., Testor, P., Bosse, A., Taupier-Letage, I., et al.,
4
5 476 (2018). Characterizing, modelling and understanding the climate variability of the deep
6
7 477 water formation in the North-Western Mediterranean Sea. *Climate Dynamics* 51, 1179–
8
9 478 1210. <https://doi.org/10.1007/s00382-016-3295-0>.
- 10
11
12 479 Soto-Navarro, J., Jordà, G., Amores, A., Cabos, W., Somot, S., Sevault, F., et al. (2020).
13
14 480 Evolution of Mediterranean Sea water properties under climate change scenarios in the
15
16 481 Med-CORDEX ensemble. *Climate Dynamics*, 54, 2135–2165.
- 17
18
19 482 Velaoras D., Papadopoulos, V. P., Kontoyianni, H., Papageorgiou, D. K., and Pavlidou,
20
21 483 A., (2017). The response of the Aegean Sea (eastern Mediterranean) to the extreme
22
23 484 2016–2017 winter. *Geophys Res Lett* 44:9416–9423.
24
25 485 <https://doi.org/10.1002/2017GL074761>
- 26
27
28 486 Velaoras D., Zervakis, V. & Theocharis, A., (2021). The physical characteristics and
29
30 487 dynamics of the Aegean water masses. In: Anagnostou C, Kostianoy A, Mariolagos I,
31
32 488 Panayotidis P, Soilemezidou M, Tsaltas G (eds) *The Aegean Sea environment: the*
33
34 489 *natural system*. Springer, DOI 10.1007/698_2020_730.
- 35
36
37 490 Wüst, G., (1961). On the vertical circulation of the Mediterranean Sea. *J. Geophys.*
38
39 491 *Res.*, 66, 3261–3271, 10.1029/JZ066i010p03261.
- 40
41
42 492 Zervakis V., Krauzig, N., Tragou, E. & Kunze, E. (2019). Estimating vertical mixing
43
44 493 in the deep North Aegean Sea using Argo data corrected for conductivity sensor drift.
45
46 494 *Deep Sea Res. Part I* 154. <https://doi.org/10.1016/j.dsr.2019.103144>

495 **Tables**

| | NWMed | Aegean Sea |
|-----------------------------|-------|------------|
| Q_e (Wm^{-2}) | -115 | -135 |
| Q_h (Wm^{-2}) | -30 | -46 |
| Q_{lw} (Wm^{-2}) | -85 | -86 |
| Q_{sw} (Wm^{-2}) | 84 | 95 |
| Q_n (Wm^{-2}) | -146 | -172 |
| u (ms^{-1}) | 7.5 | 7.1 |
| T_a ($^{\circ}C$) | 11.4 | 11.6 |
| T_s ($^{\circ}C$) | 13.5 | 14.6 |
| ΔT ($^{\circ}C$) | 2.1 | 3.0 |
| q_a ($g\ kg^{-1}$) | 6.0 | 6.1 |
| q_s ($g\ kg^{-1}$) | 9.5 | 10.2 |
| Δq ($g\ kg^{-1}$) | 3.5 | 4.1 |

496

497 Table 1 Winter (DJF) net and component heat flux means for the reference period 1951-
 498 2020 averaged over the NWMed and Aegean Sea boxes regions outlined in Fig.1a.
 499 Units Wm^{-2} . Also tabulated are the corresponding wind speed, temperature and
 500 humidity means.

501

502

503

504

505

506

507

| Decade | NCW | Convective Winters |
|-----------|-----|--|
| 1969-1978 | 6 | 1969 ^{1,2} , 1970 ^{1,2} , 1971 ¹ , 1973 ¹ , 1976 ¹ , 1978 ¹ |
| 1979-1988 | 8 | 1979 ¹ , 1980 ¹ , 1983 ¹ , 1984 ¹ , 1985 ¹ , 1986 ¹ , 1987 ^{1,3,4} , 1988 ^{1,3} |
| 1989-1998 | 4 | 1991 ³ , 1992 ^{3,5} , 1993 ¹ , 1994 ¹ |
| 1999-2008 | 4 | 1999 ^{3,7} , 2000 ³ , 2005 ³ , 2006 ^{3,7} |
| 2009-2018 | 5 | 2009 ^{6,7} , 2010 ⁶ , 2011 ⁶ , 2012 ⁶ , 2013 ^{6,7} |

508

509 Table 2 Individual convective winters by decade from 1969-1978 through 2009-2018
 510 in the NW Mediterranean Sea. NCW is the number of convective winters in each decade
 511 and has been defined according to whether, for the specific winter, there are
 512 observations, numerical models or reanalyses reported in the literature that indicate
 513 deep convection events (convection to depths ≥ 1900 m or denser than 29.0 kg m^{-3}).
 514 Reference key: 1-Mertens and Schott, 1998. 2-Gascard, 1973. 3-Pinardi et al., 2015. 4-
 515 Schott et al., 1988. 5-Rhein, 1995. 6-Margirier et al., 2018. 7-Somot et al., 2018.

516

517

518

519

520

521

522

523

524

525

1
2
3 526
4
5 527
6
7 528
8
9 529
10
11
12
13
14
15
16
17
18
19
20
21
22
23
24
25
26
27
28
29
30
31
32
33
34
35
36
37
38
39
40
41
42
43
44
45
46
47
48
49
50
51
52
53
54
55
56
57
58
59
60

Accepted Manuscript

1
2
3 531 **Figure Captions**
4

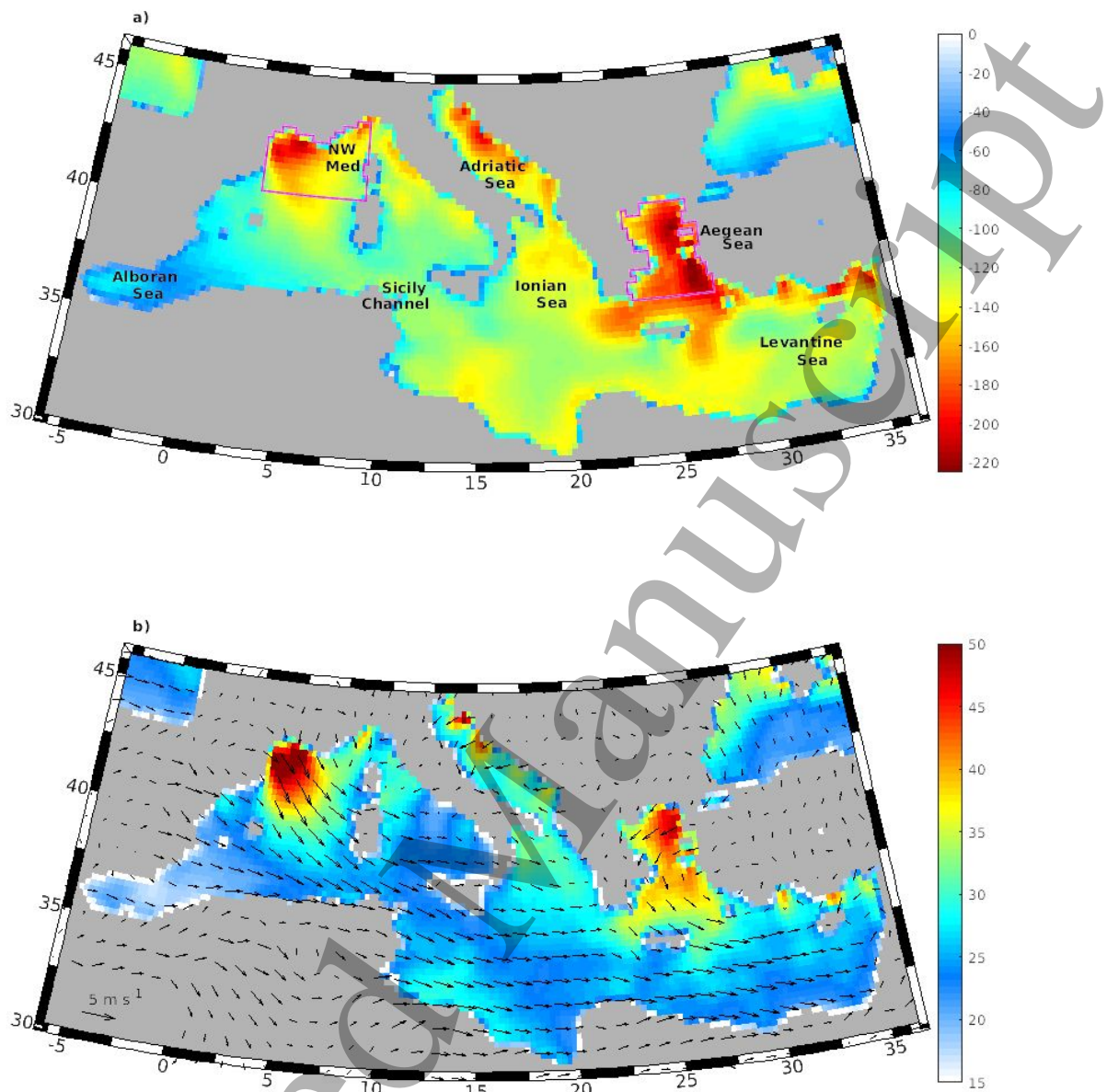
5 532 **Figure 1** a.) ERA5 1950-2020 winter mean net air-sea heat flux, Q_n , units Wm^{-2} .
6
7 533 Regions referred to in the text are labelled. Magenta outlines show the NW Med and
8
9 534 Aegean Sea boxes used for Table 1. b.) Standard deviation of individual winter mean
10
11 535 Q_n . Vectors show winter mean wind speed.

12
13
14 536 **Figure 2** a-b) Time series of ERA5 (black) and 20CRv3 (green) winter Q_n for a) the
15
16 537 NWMed and b) the Aegean. The 20CRv3 time series has been offset by the difference
17
18 538 in ERA5 and 20CRv3 winter mean Q_n for 1951-2020 in order to facilitate comparison
19
20 539 (offset value: NWMed, $-13.5 Wm^{-2}$; Aegean, $1.9 Wm^{-2}$). c-d) Distributions of
21
22 540 individual winter month Q_n using all ERA5 $0.25 \times 0.25^\circ$ grid cells within each Fig.1a box
23
24 541 for 1951-1985 (blue) and 1986-2020 (red) for c.) the NWMed and d.) the Aegean.

25
26 542 **Figure 3** a-b) Change in winter heat flux (1986-2020 minus 1951-1985) and wind speed
27
28 543 for a) the NWMed and b) the Aegean. Heat flux values (green), wind speed (black). c-
29
30 544 d) Corresponding change in temperature (red) and humidity (blue) variables for c) the
31
32 545 NWMed and d) the Aegean.

33
34 546 **Figure 4** a.) Difference (1986-2020 minus 1951-1985) of ERA5 winter 2 m air
35
36 547 temperature (coloured field, $^\circ C$) and 10 m wind speed (vectors). b.) Schematic of the
37
38 548 main changes in winter SST (orange arrows), air temperature (red arrows), sea-air
39
40 549 temperature difference (dark blue arrows) for the NWMed and Aegean. Numerical
41
42 550 values are the temperature difference (1986-2020 minus 1951-1985). Purple ellipses
43
44 551 indicate main dense water formation regions. Black arrows indicate whether winter heat
45
46 552 has loss weakened or remained unchanged in 1986-2020 relative to 1951-1985. Light
47
48 553 blue arrow shows increased cold air advection over the Aegean. Background colour
49
50 554 field is the difference sea level pressure (1986-2020 minus 1951-1985, units mb).

51
52
53
54
55
56
57
58 555
59
60

556 **Figures**

557

558 **Figure 1** a.) ERA5 1950-2020 winter mean net air-sea heat flux, Q_n , units Wm^{-2} .

559 Regions referred to in the text are labelled. Magenta outlines show the NW Med and

560 Aegean Sea boxes used for Table 1. b.) Standard deviation of individual winter mean

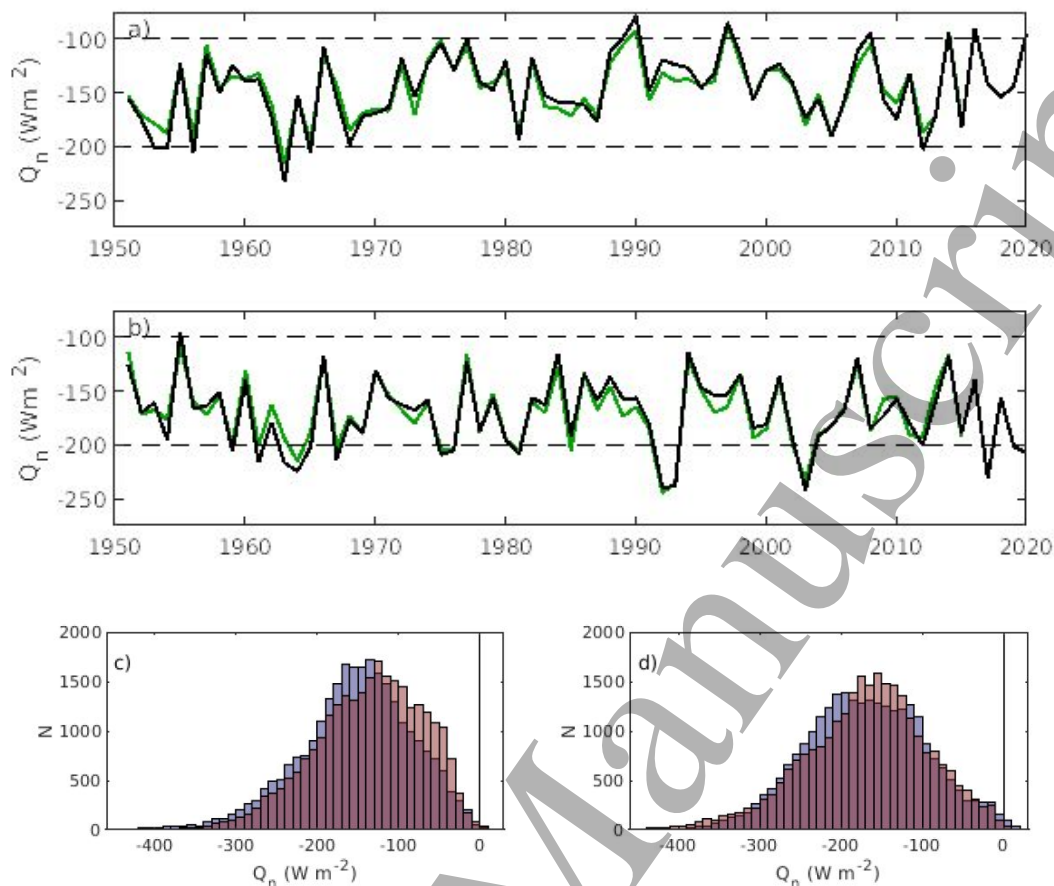
561 Q_n . Vectors show winter mean wind speed.

562

563

564

565



566

567

568

569

570

571

572

573

574

575

576

577

578

579

580

581

582

583

584

585

586

587

588

589

590

591

592

593

594

595

596

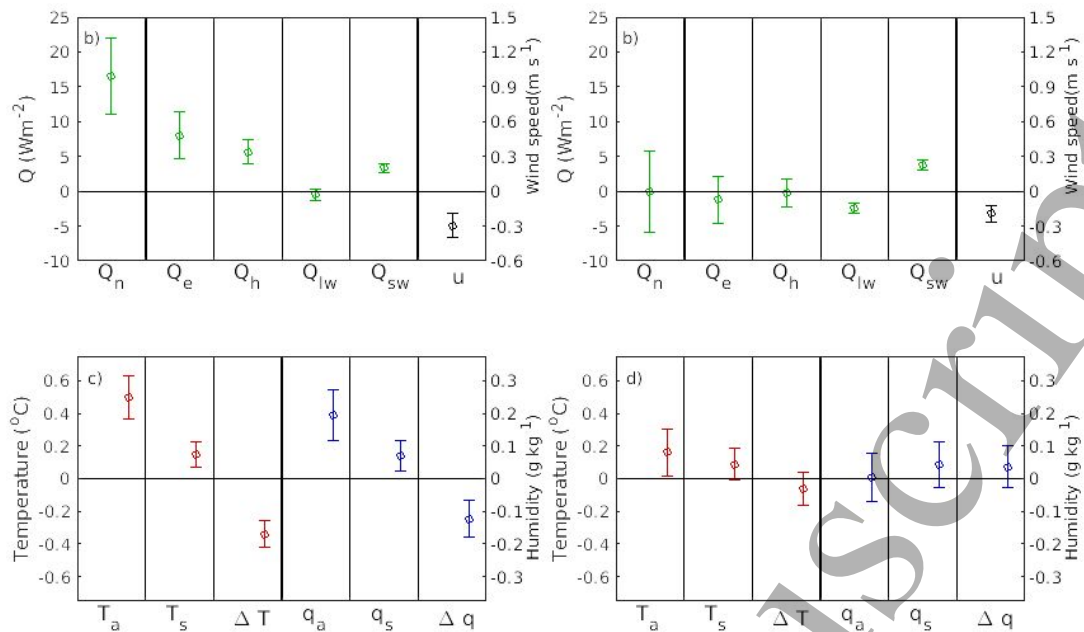
597

598

599

600

Figure 2 a-b) Time series of ERA5 (black) and 20CRv3 (green) winter Q_n for a) the NWMed and b) the Aegean. The 20CRv3 time series has been offset by the difference in ERA5 and 20CRv3 winter mean Q_n for 1951-2020 in order to facilitate comparison (offset value: NWMed, $-13.5 W m^{-2}$; Aegean, $1.9 W m^{-2}$). c-d) Distributions of individual winter month Q_n using all ERA5 $0.25 \times 0.25^\circ$ grid cells within each Fig.1a box for 1951-1985 (blue) and 1986-2020 (red) for c.) the NWMed and d.) the Aegean.



575

576 **Figure 3** a-b) Change in winter heat flux (1986-2020 minus 1951-1985) and wind speed

577 for a) the NWMed and b) the Aegean. Heat flux values (green), wind speed (black). c-

578 d) Corresponding change in temperature (red) and humidity (blue) variables for c) the

579 NWMed and d) the Aegean.

580

581

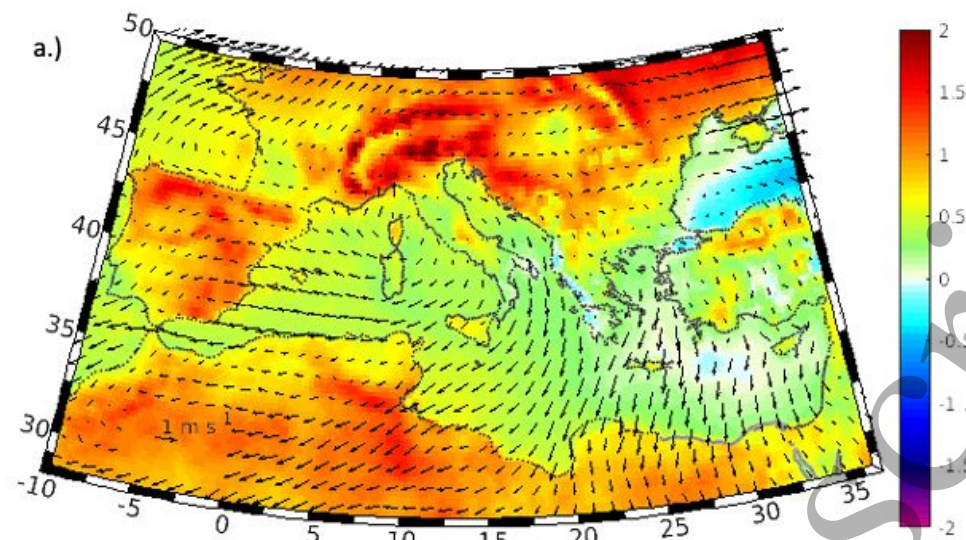
582

583

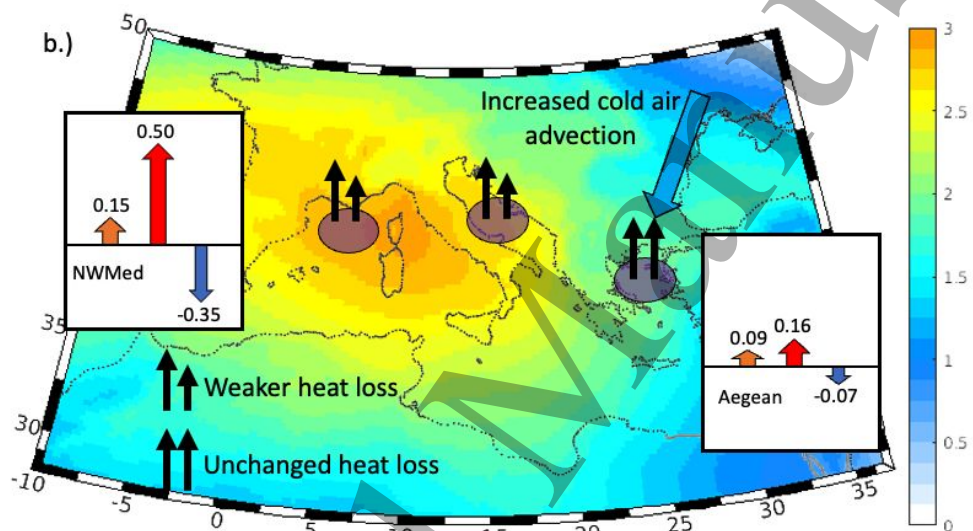
584

585

586



587



588

589 **Figure 4** a.) Difference (1986-2020 minus 1951-1985) of ERA5 winter 2 m air
 590 temperature (coloured field, °C) and 10 m wind speed (vectors). b.) Schematic of the
 591 main changes in winter SST (orange arrows), air temperature (red arrows) and sea-air
 592 temperature difference (dark blue arrows) for the NWMed and Aegean. Numerical
 593 values are the temperature difference (1986-2020 minus 1951-1985). Purple ellipses
 594 indicate main dense water formation regions. Black arrows indicate whether winter heat
 595 has loss weakened or remained unchanged in 1986-2020 relative to 1951-1985. Light
 596 blue arrow shows increased cold air advection over the Aegean. Background colour
 597 field is the sea level pressure difference (1986-2020 minus 1951-1985, units mb).